Strouhal number influence on Methane-air jet diffusion flames

M. Sánchez-Sanz[1], **B. A. V. Bennett**[2], **M. D. Smooke**[2], **A. Liñán**[1]

[1]Departamento de Motopropulsión y Termofluidomecánica
ETSI. Aeronáuticos, Universidad Politécnica de Madrid, Spain

[2]Department of Mechanical Engineering, Yale University, New Haven, USA

1 Problem formulation

In this study, we investigate computationally the effect of the variation of the oscillation frequency of the fuel inlet velocity on laminar methane-air jet diffusion flames. We have solved the transient equations for the conservation of mass, momentum, energy and species mass with detailed transport and finite-rate chemistry submodels (15 species and 42 reactions steps [1]). The equations have been integrated by using the modified vorticity-velocity formulation described in [2] and that has been used later for unteady problems in [6]. This formulation is seen to avoid problems with the mass conservation that have been previously reported in flows with strong vorticity gradients [3]. A detailed description of the computational mesh and the time-step selection can also be found at [3]. The equations are made non-dimensional by using the characteristics values of all variables at the jet exit (density ρ_F, viscosity μ_F, thermal conductivity λ_F, mass diffusivity D_F and temperature T_F), the jet radius a and the characteristic velocity U_F, yielding:

• *Radial and axial velocity equations*

$$S\,\frac{\partial}{\partial r}\left(\frac{1}{\rho}\frac{\partial \rho}{\partial t}\right)+\frac{\partial^2 v_r}{\partial r^2}+\frac{\partial^2 v_r}{\partial z^2}=\frac{\partial w}{\partial z}-\frac{1}{r}\frac{\partial v_r}{\partial r}+\frac{v_r}{r^2}-\frac{\partial}{\partial r}\left(\frac{\vec{v}\cdot\nabla\rho}{\rho}\right) \tag{1}$$

$$S\,\frac{\partial}{\partial z}\left(\frac{1}{\rho}\frac{\partial \rho}{\partial t}\right)+\frac{\partial^2 v_z}{\partial z^2}=-\frac{\partial^2 v_r}{\partial r\partial z}-\frac{1}{r}\frac{\partial v_r}{\partial z}-\frac{\partial}{\partial z}\left(\frac{\vec{v}\cdot\nabla\rho}{\rho}\right) \tag{2}$$

where ρ is the density of the mixture, $w=aw'/U_F=\partial v_r/\partial z-\partial v_z/\partial r$ the vorticity, $t=w_f t'$ the time and $z=z'/a$ and $r=r'/a$ axial and transverse coordinates respectively. The Strouhal number is defined as $S=aw_f/U_F$, with w_f the frequency of oscillation of the jet velocity . The prime $'$, here and hereafter, denotes dimensional quantities.

•*Modified vorticity equation*

$$\begin{aligned}S\left(\rho\frac{\partial w}{\partial t}+w\frac{\partial \rho}{\partial t}-\bar{\nabla}\rho\cdot\frac{\partial \vec{v}}{\partial t}\right)-\rho v_r\frac{\partial w}{\partial r}-\rho v_z\frac{\partial w}{\partial z}=&-\frac{\rho v_r}{r}\left(\frac{\partial v_r}{\partial z}-\frac{v_z}{\partial r}\right)+\bar{\nabla}\rho\cdot\nabla\left(\frac{\vec{v}\cdot\vec{v}}{2}\right)\\&+\frac{1}{Fr^2}\,\frac{\partial \rho}{\partial z}-\frac{1}{Re}\left\{2\left[\bar{\nabla}\left(\nabla\cdot\vec{v}\right)\cdot\nabla\mu-\nabla v_r\cdot\bar{\nabla}\left(\frac{\partial \mu}{\partial r}\right)-\nabla v_z\bar{\nabla}\left(\frac{\partial \mu}{\partial z}\right)\right]\right.\\&\left.+\frac{\partial^2(\mu w)}{\partial r^2}+\frac{\partial^2(\mu w)}{\partial z^2}+\frac{\partial}{\partial r}\left(\frac{\mu}{r}\frac{\partial v_r}{\partial z}\right)-\frac{\partial}{\partial r}\left(\frac{\mu}{r}\frac{\partial v_z}{\partial z}\right)\right\}\end{aligned} \tag{3}$$

Correspondence to : mario.sanchez@upm.es

where $\bar{\nabla}\beta = (\partial\beta/\partial z, \partial\beta/\partial r)$ and μ is the non-dimensional viscosity. The Froude and Reynolds numbers are defined as $Fr = U_F^2/(a\ g) = 25$ and $Re = U_F a/\nu_F = 90$ respectively.
•*Energy equation*

$$S\rho c_p \frac{\partial T}{\partial t} + \rho c_p \left(v_r \frac{\partial T}{\partial r} + v_z \frac{\partial T}{\partial z} \right) = \frac{1}{Re\ Pr} \left[\frac{1}{r} \frac{\partial}{\partial r} \left(r\lambda \frac{\partial T}{\partial r} \right) + \frac{\partial}{\partial z} \left(\lambda \frac{\partial T}{\partial r} \right) \right] + \frac{1}{Pe} \sum_{n=1}^{N_s} \rho c_{p_n} D_n \nabla Y_n \cdot \nabla T - \sum_{n=1}^{N_s} h_n \dot{w}_n + Q_r + \frac{1}{Re} \Phi_v \quad (4)$$

where λ is the thermal conductivity of the mixture, Q_r is the nondimensional radiative flux [4], Φ_v is the viscous dissipation term, c_p is the specific heat at constant pressure of the mixture and c_{p_n}, D_n, $h_n = h'_n/(c_{p_F} T_F)$ and $\dot{w}_n = \dot{w}'_n a W_n/(\rho_F U_F)$ are the specific heat at constant pressure, the mass diffusion coefficient, the enthalpy and the production rate of the *nth* species respectively, with W_n being the molecular weight. $Pr = [\lambda_F/(c_{p_F}\rho_F)]/\nu_F = 1.378$ and $Pe = aU_F/D_F = 49.14$ are Prandtl and Péclet numbers respectively.
•*Species equation,* $n \neq N_2$

$$S\rho \frac{\partial Y_n}{\partial t} + \rho v_r \frac{\partial Y_n}{\partial r} + \rho v_z \frac{\partial Y n}{\partial x} = \frac{1}{Pe} \left[\frac{1}{r} \frac{\partial}{\partial r} \left(\rho r D_n \frac{\partial Y_n}{\partial r} \right) + \frac{\partial}{\partial z} \left(\rho r D_n \frac{\partial Y_n}{\partial z} \right) \right] + \dot{w}_n \quad (5)$$

while N_2 mass fraction can be obtained by using $Y_{N_2} = 1 - \sum_{\substack{n=1 \\ n \neq N_2}}^{N_s} Y_n$. The full set of equations are discretized at all the interior points of a domain (figure 1) composed by $N_r \times N_z$ points, with $N_r = 116$ and $N_z = 162$, non-uniformly distributed ($\Delta z_{min} = \Delta r_{min} = 0.025$). The time-variation of the flow is introduced by imposing a periodic modulation of the fuel velocity at the inlet $U_0 = (1 - (r/a)^2)(1 + A \sin t)$ where the amplitude of the fluctuation is $A = 0.5$ in the computations below. The frequency of the oscillation is selected so that the Strouhal number of the flow $S = aw_f/U_F$ is equal to $S = 0.5$, 1 and 2. The velocity of the coflow $U_c = 0.5$ is introduced with a constant profile everywhere except very close to the walls where an artificial boundary layer of small thickness is included.
The computation uses as initial condition the solution obtained for a steady flame previously computed. The calculation continues until the solution attains a periodically steady solution in which the differences between the results obtained for two consecutive cycles fall below a certain value. The time step is adaptively chosen based on the condition that the CFL number cannot exceed a limiting value of 0.7 and typically varies between $\Delta t = 0.001$ and $\Delta t = 0.01$.
With regard to the boundary conditions, at the centerline $r = 0$ symmetry conditions are imposed $v_r = \partial Y_n/\partial r = \partial u_z/\partial r = \partial w/\partial r = 0$ while at $r = R_{max}$ we impose vanishing radial gradients for velocity, temperature and species $\partial u_z/\partial r = \partial u_r/\partial r = \partial T/\partial r = \partial Y_n/\partial r = 0$. At the outflow, axial gradients of the variables vanish as well while at $z = 0$ we impose $u_z = U_0$, $u_r = 0$, $T = T_0$, $Y_{CH_4} = 0.5149$, $Y_{N_2} = 0.4852$ for $r < 1$, $u_r = 0$, $T = T_0$, $Y_{O_2} = 0.232$, $Y_{N_2} = 0.768$ for $r > 1$ with $u_z = U_c$ if $1 < r < b$ and $u_z = 0$ otherwise.

2 Result and discussion

The unsteadiness introduced by the velocity modulation affects both the fluid dynamic and the chemistry of the problem. The pulsation induced the creation of outer vortices that interact with the flame perturbing not only its shape but also its chemical structure. Profiles of CH_4, CO, CO_2, O_2 and H_2O together with the CH_4 consumption rate have been plotted at the centerline in figure 2 for a pulsation amplitude $A = 0.5$ and different Strouhal numbers. Each of the panels represents a different time within an oscillation cycle $t = 0$ and $t = 0.5$.

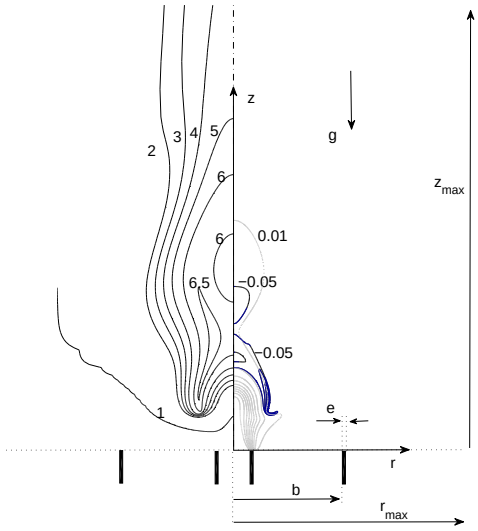

Figure 1: Coordinate system and geometry considered in the calculation. In the computation we have used $b = b'/a = 12.5$, $e = e'/a = 0.1$, $r_{max} = r'_{max}/a = 37.5$ and $z_{max} = z'_{max}/a = 100$. The acceleration due to gravity g acts in z direction pointing toward decreasing values of the axial coordinate. This sample calculation shows temperature T in the left half of the plot, for $A = 0.5$ and $S = 0.5$ at $t = 0.45$, while CH_4 consumption rate $\bar{w}_{CH_4} = \dot{w}_{CH_4}/Y_{F_0}$ (solid line) and Y_{CH_4} (dotted line) are shown in the right half of the plot. Six and nine equally spaced contours are plotted for $\bar{w}_{CH_4}$ between -0.05 and -0.3 and Y_{CH_4} between 0.01 and 0.91 respectively. Temperature isocontours are specified in the figure.

The effect of the unsteadiness is clear when we compared the evolution of the mass fraction of different species at the centerline with the steady solution. The differences are specially important for Y_{CH_4}, Y_{CO} and Y_{CO2}, with variations in both the intensity and the location of the concentration peaks during the course of a cycle due to stretch and strain effects of the outer vortex created during the pulsation. These vortices, with large transverse velocity, collide with the flame surface. As the methane flame is pushed radially outward or inward, the flame temperature changes, decreasing as the flame is stretched and increasing when it is compressed. As a consequence of this temperature variation, the consumption and production rates of the species involved in the reaction are modified, leading to strong changes in their concentrations. To check this effect we have plotted the methane consumption rate. At the beginning of the cycle, the largest values of $\dot{w}_{CH_4}$ occur at approximately the same location independently of the value of S. As the flame/vortex interaction becomes more intense, the differences between the oscillation frequencies are more evident. Specially remarkable is what happen in panel (b) of figure 2; for $S = 0.5$ the vortex has stretched the flame so intensely that the reaction ends up quenching, generating two reaction regions separated by a gap where no reaction occurs. Shortly after that, the vortex moves away allowing the flame to be lighted again as the hot gases coming from upstream occupied the region where the vortex was located. An example of the same situation can also be observed in the isocontour plot of figure 1.

The changes in the concentration of the different species depends strongly on the frequency of oscillation. From figure 2 it can be observed differences over 50% for the mass fraction of CH_4, CO and CO_2 for $S = 0.5$ when compared with the steady solution. As the Strouhal number is increased, the differences almost disappear for $S = 2$. The distance that the perturbation introduced by the modulation in the fuel velocity can travel downstream is fundamental to understanding this behavior. The non-steady component of the solution decays rapidly as we move toward larger values of the axial coordinate, with a factor that depends on the Strouhal number of the modulation. A larger value of S is translated in

faster decay rates, making the perturbation to disappear before reaching the lift-off height of the flame, not affecting the chemistry and leaving unchanged temperature and species concentration.
As reported in previous experimental works [5], the CO mass fraction reaches values that are higher than those obtained for the steady flame, being possible to observe values over 15% higher for $S = 0.5$. It has been suggested [6] that the inhibition of the oxidation reaction $CO + OH \rightarrow CO_2 + H$ is the responsible for the detected increment, but further investigation must be done to understand the effect of the frequency of oscillation on CO emissions.

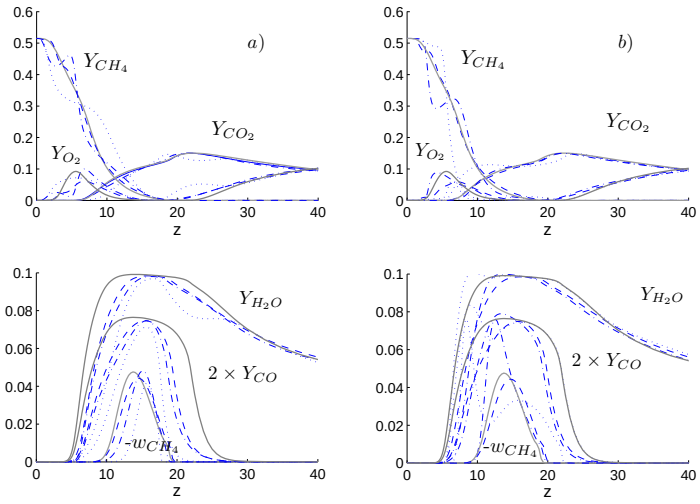

Figure 2: Mass fraction and scaled CH_4 production rate $\bar{w}_{CH_4} = \dot{w}_{CH_4}/Y_F$ along the centerline at different times within the oscillation cycle $t = 0$ (a) and $t = 0.5$ (b) for $A = 0.5$ and $S = 0.5$ (dotted line), $S = 1$ (dot-dashed line), $S = 2$ (dashed line). The solid line corresponds to the solution for the steady flame.

References

[1] Smooke M.D., Mitchell R.E., Keyes D.E. Numerical solution of two-dimensional axisymmetric laminar diffusion flames. Combust. Sci. Tech. 67: 85.

[2] Dworkin S. B., Bennett B.A.V., Smooke M.D. (2006). A mass-conserving vorticity-velocity formulation with application to nonreacting and reacting flows. J. Comput. Phys. 215,: 430.

[3] A. Ern. Vorticity-velocity modeling of chemically reacting flows. PhD thesis, Yale University, Mechanical Engineering Department (1994).

[4] Hall R. J.. (1993). The radiative dissipation in planar gas-soot mixtures. Quantum J. Spectrosco. Radiat. Transfer, 51: 635.

[5] Everest D.A., Shaddix C.R., Smyth K.C. (1996). Quantitative two-photon laser-induced fluorescence imaging of CO in flickering CH_4/air diffusion flames. Proc. Combust. Inst: 1161.

[6] Dworkin S. B, B.C. Connelly, AM. Schaffer, B.A.V. Bennett, M.B. Long, M.D. Smooke, M.P. Puccio, B. McAdrews, J.H. Miller (2007). Computational and experimental study of a forced, time-dependent, methane-air coflow diffusion flame, Proc. Combust. Inst. 31: 971.